PRODUCTION OF LARGE TRANSVERSE MOMENTUM W BOSONS AT THE TEVATRON

Nikolaos Kidonakis[1] and Agustín Sabio Vera[2]

[1] *Kennesaw State University, 1000 Chastain Rd., #1202*
Kennesaw, GA 30144–5591, USA
[2] *II. Institut für Theoretische Physik, Universität Hamburg,*
Luruper Chaussee 149, 22761 Hamburg, Germany

ABSTRACT

We discuss the production of W bosons at large transverse momentum in $p\bar{p}$ collisions at the Tevatron Run I and II. W boson hadroproduction is a process of relevance in testing the Standard Model and in estimates of backgrounds to new physics. The next–to–leading order cross section in the region of large transverse momentum is dominated by threshold soft–gluon corrections which arise from incomplete cancellations near partonic threshold between graphs with real emission and virtual graphs due to the limited phase space available for real gluon emission. In this contribution it is shown how, by including next–to–next–to–leading–order (NNLO) soft-gluon corrections, the transverse momentum distribution of the W at the Tevatron is modestly enhanced and the dependence on the factorization and renormalization scales is significantly reduced.

1   INTRODUCTION

At hadron–hadron colliders a process of major relevance is the production of W bosons in the electroweak sector. Such a scattering process serves as a direct test of the Standard Model and as an estimate of backgrounds to possible new physical phenomena. A significant example is $Wb\bar{b}$ production, the principal background to the associated Higgs boson production $p\bar{p} \to H(\to b\bar{b})W$ at the Tevatron [1].

The full next–to–leading-order (NLO) calculation of the cross section for W hadroproduction at large transverse momentum was first presented in Refs. [2, 3]. The results in that work showed that the differential distributions in transverse momentum Q_T of the W boson are enhanced with respect to the leading order (LO) calculation. This Q_T distribution falls rapidly with increasing Q_T, spanning five orders of magnitude in the 30 GeV $< Q_T <$ 190 GeV region at the Tevatron. As expected from a consistent perturbative expansion, the NLO corrections also considerably stabilize the dependence of the cross section on the factorization and renormalization scales.

When a hard–scattering cross section takes place close to the partonic threshold, as is the case in high transverse momentum production of electroweak bosons, corrections related to the emission of soft gluons from the partons in the process have to be taken into account. Near partonic threshold there are incomplete cancellations between real emission graphs and virtual ones, generating, at each order in perturbation theory, large logarithms stemming from the limited phase space available for real gluon emission near threshold. When these threshold corrections are calculated in the eikonal approximation they exponentiate as a consequence of the factorization properties [4, 5, 6] of the cross section. In general terms the factorization of the cross section is done in terms of functions which describe those gluons collinear to the incoming partons, hard quanta, and noncollinear soft–gluons. The renormalization group properties of such functions result in resummation. The threshold corrections have by now been successfully resummed for many processes [7].

In this chapter the resummation of threshold logarithms together with the expansion of the resummed cross section at next–to–next–to–leading order (NNLO) for electroweak W boson hadroproduction, which was first presented in Ref. [8] at next–to–next–to–leading logarithmic (NNLL) accuracy, are further studied. We note that in Ref. [8] no numerical phenomenological studies were made.

Quite recently, an approach which unifies the calculation of NNLO soft and virtual corrections for hadron–hadron and lepton–hadron processes has been presented in Ref. [9]. This work puts together and extends previous approaches by going beyond NNLL accuracy. In this chapter that work is closely followed to calculate the NNLO soft corrections to W production at large transverse momentum at the Tevatron. The theoretical results presented here are consistent with those in Ref. [8] although they slightly differ in that the transverse momentum Q_T is now used as the hard scale instead of the mass of the W.

This chapter is based on the work of Ref. [10] where we studied the significance of NNLO soft–gluon corrections for W–boson production at large transverse momentum. The accuracy of the theoretical calculation is increased to next–to–next–to–next–to–leading logarithms (NNNLL). We note that we work in the $\overline{\text{MS}}$ scheme throughout.

The present results are closely related to previous studies of direct photon production, for which numerical analysis were presented in Ref. [11]. The relation arises because the partonic subprocesses involved in direct photon production are similar to the ones discussed in this chapter.

In Section 2 the kinematics of the partonic subprocesses involved is discussed and the corrections to be calculated are defined. In Section 3 results for the NLO soft and virtual, and the NNLO soft–gluon corrections are provided. It is shown how the NLO soft corrections agree near partonic threshold with the exact NLO calculations of Refs. [2, 3] while our NNLO soft–gluon corrections provide new predictions. In Section 4 we study the numerical effect of the NNLO soft–gluon corrections to W hadroproduction at the Tevatron Run I and II, while also showing that the NLO cross section is dominated by soft–gluon corrections.

2   KINEMATICS FOR W PRODUCTION IN HADRON COLLISIONS

We study the production of a W boson, with mass m_W, in collisions of hadron h_A with hadron h_B,

$$h_A(P_A) + h_B(P_B) \longrightarrow W(Q) + X \,, \tag{2.1}$$

where X denotes any allowed additional final-state particles. At the parton level, the lowest–order subprocesses for the production of a W boson and a parton are

$$
\begin{aligned}
q(p_a) + g(p_b) &\longrightarrow W(Q) + q(p_c)\,, \\
q(p_a) + \bar{q}(p_b) &\longrightarrow W(Q) + g(p_c)\,.
\end{aligned}
\tag{2.2}
$$

We can write the factorized single–particle–inclusive cross section as

$$
\begin{aligned}
E_Q \,\frac{d\sigma_{h_A h_B \to W(Q)+X}}{d^3Q} \;=\; & \sum_f \int dx_1 \, dx_2 \; \phi_{f_a/h_A}(x_1, \mu_F^2) \, \phi_{f_b/h_B}(x_2, \mu_F^2) \\
& \times E_Q \,\frac{d\hat{\sigma}_{f_a f_b \to W(Q)+X}}{d^3Q}(s, t, u, Q, \mu_F, \alpha_s(\mu_R^2))
\end{aligned}
\tag{2.3}
$$

where $E_Q = Q^0$, $\phi_{f/h}(x)$ is the parton distribution for parton f carrying a momentum fraction x in hadron h, and $\hat{\sigma}$ is the perturbative parton–level cross section. The initial–state collinear singularities are factorized into the parton distributions at factorization scale μ_F, while μ_R is the renormalization scale.

The hadronic and partonic kinematical invariants in the process are

$$
\begin{aligned}
S &= (P_A + P_B)^2, \\
T &= (P_A - Q)^2, \\
U &= (P_B - Q)^2, \\
S_2 &= S + T + U - Q^2, \\
s &= (p_a + p_b)^2, \\
t &= (p_a - Q)^2, \\
u &= (p_b - Q)^2, \\
s_2 &= s + t + u - Q^2,
\end{aligned}
\tag{2.4}
$$

where S_2 and s_2 are the invariant masses of the system recoiling against the electroweak boson at the hadron and parton levels, respectively. The invariant $s_2 = (p_a + p_b - Q)^2$ parametrizes the inelasticity of the parton scattering, taking the value $s_2 = 0$ at partonic threshold. Since x_i is the initial–parton momentum fraction, defined by $p_a = x_1 P_A$ and $p_b = x_2 P_B$, the hadronic and partonic kinematical invariants are related by

$$
\begin{aligned}
s &= x_1 x_2 S, \\
t - Q^2 &= x_1 (T - Q^2) \\
u - Q^2 &= x_2 (U - Q^2).
\end{aligned}
\tag{2.5}
$$

We note that for numerical calculations it is convenient to write the hadronic kinematical variables T and U in the alternative way

$$
\begin{aligned}
T &= m_W^2 - m_T \sqrt{S} e^{-y} \\
U &= m_W^2 - m_T \sqrt{S} e^{y},
\end{aligned}
\tag{2.6}
$$

where m_W is the mass of the W boson, $m_T = \sqrt{Q_T^2 + m_W^2}$ is its transverse mass, and y is its rapidity. With this notation the differential Q_T distribution can then be expressed as

$$
\frac{d\sigma_{h_A h_B \to W+X}}{dQ_T^2} \left(S, m_W^2, Q_T \right) = \sum_f \int_0^1 dy' \int_A^1 dx_1 \int_0^{s_2^{\max}} ds_2 \frac{2\pi Y}{x_1 S - \sqrt{S} m_T e^y}
\tag{2.7}
$$

$$
\times \phi_{f_a/h_A} \left(x_1, \mu_F^2 \right) \phi_{f_b/h_B} \left(x_2, \mu_F^2 \right) E_Q \frac{d\hat{\sigma}_{f_a f_b \to W+X}}{d^3 Q} \left(x_1, x_2, y \right),
$$

where the relations $Y = \ln \left(B + \sqrt{B^2 - 1} \right)$, $B = (S + m_W^2)/(2 m_T \sqrt{S})$, and $y = Y(2y' - 1)$, hold. The kinematical limits of the integrations read

$$
s_2^{\max} = m_W^2 - \sqrt{S} m_T e^y + x_1 \left(S - \sqrt{S} m_T e^{-y} \right),
\tag{2.8}
$$

$$
A = \frac{\sqrt{S} m_T e^y - m_W^2}{S - \sqrt{S} m_T e^{-y}}, \quad x_2 = \frac{s_2 - m_W^2 + \sqrt{S} m_T x_1 e^{-y}}{x_1 S - \sqrt{S} m_T e^y}.
\tag{2.9}
$$

In general, the partonic cross section $\hat{\sigma}$ includes distributions with respect to s_2 at n–th order in the strong coupling α_s of the type

$$
\left[\frac{\ln^m (s_2/Q_T^2)}{s_2} \right]_+, \qquad m \leq 2n - 1,
\tag{2.10}
$$

defined by their integral with any smooth function f by

$$
\int_0^{s_2\,max} ds_2 \, f(s_2) \left[\frac{\ln^m (s_2/Q_T^2)}{s_2} \right]_+ \equiv
$$

$$
\int_0^{s_2\,max} ds_2 \frac{\ln^m (s_2/Q_T^2)}{s_2} [f(s_2) - f(0)] + \frac{1}{m+1} \ln^{m+1} \left(\frac{s_2\,max}{Q_T^2} \right) f(0).
\tag{2.11}
$$

3

These "plus" distributions are the remnants of cancellations between real and virtual contributions to the cross section. Note that in Ref. [8] Q was used instead of Q_T in the plus distributions. Here we prefer to use Q_T as we find it a slightly better physical hard scale for the Q_T distributions that we will be calculating. Below we will make use of the terminology that at n–th order in α_s the leading logarithms (LL) are those with $m = 2n-1$ in Eq. (2.10), next–to–leading logarithms (NLL) with $m = 2n - 2$, next–to–next–to–leading logarithms (NNLL) with $m = 2n - 3$, and next–to–next–to–next–to–leading logarithms (NNNLL) with $m = 2n - 4$.

3   NEXT–TO–NEXT–TO–LEADING ORDER SOFT–GLUON CORRECTIONS

In this section, we first present the NLO soft and virtual corrections for each of the subprocesses in Eq. (2.2). We then present the NNLO soft and some virtual corrections.

3.1   NLO and NNLO corrections for $qg \longrightarrow Wq$

We begin with the $qg \longrightarrow Wq$ subprocess. The Born differential cross section for this process is

$$E_Q \frac{d\sigma^B_{qg \to Wq}}{d^3Q} = F^B_{qg \to Wq}\, \delta(s_2)\,, \tag{3.1}$$

where

$$F^B_{qg \to Wq} = \frac{\alpha\, \alpha_s(\mu_R^2)C_F}{s(N_c^2 - 1)} A^{qg} \sum_f |L_{ff_a}|^2\,, \tag{3.2}$$

$$A^{qg} = -\left(\frac{s}{t} + \frac{t}{s} + \frac{2uQ^2}{st}\right)\,,$$

with L the left–handed couplings of the W boson to the quark line, f the quark flavor and $\sum_f$ the sum over the flavors allowed by the CKM mixing and by the energy threshold. For the L couplings we choose the conventions of Ref. [3]. Also $C_F = (N_c^2 - 1)/(2N_c)$ with $N_c = 3$ the number of colors.

We can write the NLO soft and virtual corrections for $qg \longrightarrow Wq$ in single–particle inclusive kinematics as

$$E_Q \frac{d\hat\sigma^{(1)}_{qg \to Wq}}{d^3Q} = F^B_{qg \to Wq} \frac{\alpha_s(\mu_R^2)}{\pi} \left\{ c_3^{qg} \left[\frac{\ln(s_2/Q_T^2)}{s_2}\right]_+ + c_2^{qg} \left[\frac{1}{s_2}\right]_+ + c_1^{qg}\, \delta(s_2) \right\}\,. \tag{3.3}$$

Note that the $[\ln(s_2/Q_T^2)/s_2]_+$ term (which is the LL, since $m = n = 1$ in Eq. (2.10)) and the $[1/s_2]_+$ term (NLL, since $n = 1$, $m = 0$) are the soft gluon corrections. The $\delta(s_2)$ term is the contribution from the virtual corrections. Below we use the terminology "NLO–NLL" to indicate when, at next–to–leading order, we include the LL and NLL soft–gluon terms (as well as scale-dependent terms in $\delta(s_2)$). Also the terminology "soft and virtual" is used to denote all the terms in Eq. (3.3). As we will see, we need to know both soft and virtual corrections at NLO in order to derive the soft terms at NNLO with at least NNLL accuracy.

The NLO coefficients in Eq. (3.3) are $c_3^{qg} = C_F + 2C_A$,

$$c_2^{qg} = -(C_F + C_A) \ln\left(\frac{\mu_F^2}{Q_T^2}\right) - \frac{3}{4}C_F - C_A \ln\left(\frac{tu}{sQ_T^2}\right)\,, \tag{3.4}$$

and

$$c_1^{qg} = \frac{1}{2A^{qg}} \left[B_1^{qg} + B_2^{qg}n_f + C_1^{qg} + C_2^{qg}n_f\right] + \frac{c_3^{qg}}{2} \ln^2\left(\frac{Q_T^2}{Q^2}\right) + c_2^{qg} \ln\left(\frac{Q_T^2}{Q^2}\right)\,, \tag{3.5}$$

4

with $C_A = N_c$, $n_f = 5$ the number of light quark flavors, and B_1^{qg}, B_2^{qg}, C_1^{qg}, and C_2^{qg} as given in the Appendix of Ref. [3] but without the renormalization counterterms and using $f_A \equiv \ln(A/Q^2) = 0$.

Note that we can write $c_2^{qg} \equiv c_{2\,\mu}^{qg} + T_2^{qg}$ with $c_{2\,\mu}^{qg} \equiv -(C_F + C_A)\ln(\mu_F^2/s)$. Similarly we also write $c_1^{qg} \equiv c_{1\,\mu}^{qg} + T_1^{qg}$ with

$$c_{1\,\mu}^{qg} \equiv \ln\left(\frac{\mu_F^2}{s}\right)\left[-\frac{\beta_0}{4} + C_F\left(\ln\left(\frac{-u}{Q_T^2}\right) - \frac{3}{4}\right) + C_A\ln\left(\frac{-t}{Q_T^2}\right)\right] + \frac{\beta_0}{4}\ln\left(\frac{\mu_R^2}{s}\right), \quad (3.6)$$

where $\beta_0 = (11C_A - 2n_f)/3$ is the lowest–order beta function. Thus, $c_{2\,\mu}^{qg}$ and $c_{1\,\mu}^{qg}$ are scale–dependent parts of the c_2^{qg} and c_1^{qg} coefficients, respectively, while T_2^{qg} and T_1^{qg} are scale–independent parts. We have kept the factorization scale μ_F and the renormalization scale μ_R separate. Finally, another useful notation is $c_1^{qg} \equiv c_{1\,\mu}'^{qg} + T_1'^{qg}$ where $c_{1\,\mu}'^{qg}$ is defined as $c_{1\,\mu}^{qg}$ with Q_T^2 instead of s in the denominators of the logarithms involving the scales μ_F and μ_R.

Using the above conventions, the NNLO soft corrections for $qg \longrightarrow Wq$ can be written as

$$E_Q\frac{d\hat{\sigma}_{qg\to Wq}^{(2)}}{d^3Q} = F_{qg\to Wq}^B\,\frac{\alpha_s^2(\mu_R^2)}{\pi^2}\,\hat{\sigma}_{qg\to Wq}'^{(2)} \quad (3.7)$$

with

$$
\begin{aligned}
\hat{\sigma}_{qg\to Wq}'^{(2)} =\;& \frac{1}{2}(c_3^{qg})^2\left[\frac{\ln^3(s_2/Q_T^2)}{s_2}\right]_+ + \left[\frac{3}{2}c_3^{qg}\,c_2^{qg} - \frac{\beta_0}{4}c_3^{qg} + C_F\frac{\beta_0}{8}\right]\left[\frac{\ln^2(s_2/Q_T^2)}{s_2}\right]_+ \\
&+ \left\{c_3^{qg}\,c_1^{qg} + (c_2^{qg})^2 - \zeta_2\,(c_3^{qg})^2 - \frac{\beta_0}{2}T_2^{qg} + \frac{\beta_0}{4}c_3^{qg}\ln\left(\frac{\mu_R^2}{s}\right) + (C_F + C_A)\,K \right. \\
&\left. + C_F\left[-\frac{K}{2} + \frac{\beta_0}{4}\ln\left(\frac{Q_T^2}{s}\right)\right] - \frac{3}{16}\beta_0 C_F\right\}\left[\frac{\ln(s_2/Q_T^2)}{s_2}\right]_+ \\
&+ \left\{c_2^{qg}\,c_1^{qg} - \zeta_2\,c_2^{qg}\,c_3^{qg} + \zeta_3\,(c_3^{qg})^2 - \frac{\beta_0}{2}T_1^{qg} + \frac{\beta_0}{4}c_2^{qg}\ln\left(\frac{\mu_R^2}{s}\right) + \mathcal{G}_{qg}^{(2)}\right. \\
&+ (C_F + C_A)\left[\frac{\beta_0}{8}\ln^2\left(\frac{\mu_F^2}{s}\right) - \frac{K}{2}\ln\left(\frac{\mu_F^2}{s}\right)\right] - C_F\,K\ln\left(\frac{-u}{Q_T^2}\right) - C_A\,K\ln\left(\frac{-t}{Q_T^2}\right) \\
&\left. + C_F\left[\frac{\beta_0}{8}\ln^2\left(\frac{Q_T^2}{s}\right) - \frac{K}{2}\ln\left(\frac{Q_T^2}{s}\right)\right] - \frac{3}{16}\beta_0 C_F\ln\left(\frac{Q_T^2}{s}\right)\right\}\left[\frac{1}{s_2}\right]_+, \quad (3.8)
\end{aligned}
$$

where $K = C_A(67/18 - \zeta_2) - 5n_f/9$ is a two–loop function in the $\overline{\text{MS}}$ scheme [12], $\zeta_2 = \pi^2/6$ and $\zeta_3 = 1.2020569\cdots$ are Riemann zeta functions, $\beta_1 = 34C_A^2/3 - 2n_f(C_F + 5C_A/3)$ is the next–to–leading order beta function, and

$$\gamma_{q/q}'^{(2)} = C_F^2\left(\frac{3}{32} - \frac{3}{4}\zeta_2 + \frac{3}{2}\zeta_3\right) + C_F C_A\left(-\frac{3}{4}\zeta_3 + \frac{11}{12}\zeta_2 + \frac{17}{96}\right) + n_f C_F\left(-\frac{\zeta_2}{6} - \frac{1}{48}\right), \quad (3.9)$$

$$\gamma_{g/g}'^{(2)} = C_A^2\left(\frac{2}{3} + \frac{3}{4}\zeta_3\right) - n_f\left(\frac{C_F}{8} + \frac{C_A}{6}\right), \quad (3.10)$$

are two–loop parton anomalous dimensions [13, 14].

The LL are the $[\ln^3(s_2/Q_T^2)/s_2]_+$ term (since $n = 2$, $m = 3$ in Eq. (2.10)), the NLL are the $[\ln^2(s_2/Q_T^2)/s_2]_+$ term ($n = 2$, $m = 2$), the NNLL are the $[\ln(s_2/Q_T^2)/s_2]_+$ term ($n = 2$, $m = 1$), and the NNNLL are the $[1/s_2]_+$ term ($n = 2$, $m = 0$). The function $\mathcal{G}_{qg}^{(2)}$ in the NNNLL term denotes a set of two–loop contributions [15] and is given by [9, 10]

$$
\begin{aligned}
\mathcal{G}_{qg}^{(2)} =\;& C_F^2\left(-\frac{3}{32} + \frac{3}{4}\zeta_2 - \frac{3}{2}\zeta_3\right) + C_F C_A\left(\frac{3}{4}\zeta_3 - \frac{11}{12}\zeta_2 - \frac{189}{32}\right) \\
&+ C_A^2\left(\frac{7}{4}\zeta_3 + \frac{11}{3}\zeta_2 - \frac{41}{216}\right) + n_f C_F\left(\frac{1}{6}\zeta_2 + \frac{17}{16}\right) + n_f C_A\left(-\frac{2}{3}\zeta_2 - \frac{5}{108}\right). \quad (3.11)
\end{aligned}
$$

Note that we have not included in $\mathcal{G}_{qg}^{(2)}$ two–loop process–dependent contributions. These additional contributions have to be included for a full NNNLL calculation. However from related studies for other processes, including top hadroproduction [16] and direct photon production [11] we expect such contributions to be small. It is actually the $-\zeta_2 c_2^{qg} c_3^{qg} + \zeta_3 (c_3^{qg})^2$ terms in Eq. (3.12) that provide the major contribution to the NNNLL term.

We use the terminology "NNLO–NNLL" below, to indicate that we include the LL, NLL, and NNLL terms at NNLO, while we use "NNLO–NNNLL" to indicate that in addition we include the NNNLL terms as well.

We remind the reader that here we do not calculate the full NNLO virtual corrections, proportional to $\delta(s_2)$. However, we have calculated explicitly here all the $\delta(s_2)$ terms that include the factorization and renormalization scale–dependence. Note that when discussing scale dependence at NNLO–NNNLL we include all scale–dependent $\delta(s_2)$ terms, which is a consistent approach from the resummation procedure [16]. These terms are

$$
\begin{aligned}
&\left\{ \frac{1}{2}(c'^{qg}_{1\,\mu})^2 + c'^{qg}_{1\,\mu} T'^{qg}_1 + \frac{\beta_0}{4} c'^{qg}_{1\,\mu} \ln\left(\frac{Q_T^2}{s}\right) + \frac{\beta_0}{4} c_1^{qg} \ln\left(\frac{\mu_R^2}{Q_T^2}\right) - (C_F + C_A)^2 \frac{\zeta_2}{2} \ln^2\left(\frac{\mu_F^2}{Q_T^2}\right) \right. \\
&+ (C_F + C_A) \ln\left(\frac{\mu_F^2}{Q_T^2}\right) \left(\zeta_2 T_2^{qg} - \zeta_2 (C_F + C_A) \ln\left(\frac{Q_T^2}{s}\right) - \zeta_3 c_3^{qg} \right) \\
&- \frac{\beta_0^2}{32} \ln^2\left(\frac{\mu_R^2}{Q_T^2}\right) - \frac{\beta_0^2}{16} \ln\left(\frac{\mu_R^2}{Q_T^2}\right) \ln\left(\frac{Q_T^2}{s}\right) + \frac{\beta_1}{16} \ln\left(\frac{\mu_R^2}{Q_T^2}\right) \\
&+ \frac{\beta_0}{8} \left[\frac{3}{4} C_F + \frac{\beta_0}{4} - C_F \ln\left(\frac{-u}{Q_T^2}\right) - C_A \ln\left(\frac{-t}{Q_T^2}\right) \right] \left[\ln^2\left(\frac{\mu_F^2}{Q_T^2}\right) + 2 \ln\left(\frac{\mu_F^2}{Q_T^2}\right) \ln\left(\frac{Q_T^2}{s}\right) \right] \\
&+ C_F \frac{K}{2} \ln\left(\frac{-u}{Q_T^2}\right) \ln\left(\frac{\mu_F^2}{Q_T^2}\right) + C_A \frac{K}{2} \ln\left(\frac{-t}{Q_T^2}\right) \ln\left(\frac{\mu_F^2}{Q_T^2}\right) \\
&\left. - (\gamma'^{(2)}_{q/q} + \gamma'^{(2)}_{g/g}) \ln\left(\frac{\mu_F^2}{Q_T^2}\right) \right\} \delta(s_2)\,.
\end{aligned}
\tag{3.12}
$$

3.2   NLO and NNLO corrections for $q\bar{q} \longrightarrow Wg$

Next, we study the partonic subprocess $q\bar{q} \longrightarrow Wg$. The Born differential cross section is

$$
E_Q \frac{d\sigma^B_{q\bar{q}\to Wg}}{d^3Q} = F^B_{q\bar{q}\to Wg}\, \delta(s_2)\,,
\tag{3.13}
$$

where

$$
\begin{aligned}
F^B_{q\bar{q}\to Wg} &= \frac{\alpha \alpha_s(\mu_R^2) C_F}{s N_c} A^{q\bar{q}} |L_{f_b f_a}|^2\,, \tag{3.14} \\
A^{q\bar{q}} &= \frac{u}{t} + \frac{t}{u} + \frac{2Q^2 s}{tu}\,.
\end{aligned}
$$

The NLO soft and virtual corrections in single–particle inclusive kinematics can be written as

$$
E_Q \frac{d\hat{\sigma}^{(1)}_{q\bar{q}\to Wg}}{d^3Q} = F^B_{q\bar{q}\to Wg} \frac{\alpha_s(\mu_R^2)}{\pi} \left\{ c_3^{q\bar{q}} \left[\frac{\ln(s_2/Q_T^2)}{s_2} \right]_+ + c_2^{q\bar{q}} \left[\frac{1}{s_2} \right]_+ + c_1^{q\bar{q}} \delta(s_2) \right\}\,.
\tag{3.15}
$$

Here the NLO coefficients are $c_3^{q\bar{q}} = 4C_F - C_A$,

$$
c_2^{q\bar{q}} = -2C_F \ln\left(\frac{\mu_F^2}{Q_T^2}\right) - (2C_F - C_A) \ln\left(\frac{tu}{sQ_T^2}\right) - \frac{\beta_0}{4}
\tag{3.16}
$$

and

$$
c_1^{q\bar{q}} = \frac{1}{2A^{q\bar{q}}} \left[B_1^{q\bar{q}} + C_1^{q\bar{q}} + (B_2^{q\bar{q}} + D_{aa}^{(0)}) n_f \right] + \frac{c_3^{q\bar{q}}}{2} \ln^2\left(\frac{Q_T^2}{Q^2}\right) + c_2^{q\bar{q}} \ln\left(\frac{Q_T^2}{Q^2}\right)\,,
\tag{3.17}
$$

6

with $B_1^{q\bar{q}}$, $B_2^{q\bar{q}}$, $C_1^{q\bar{q}}$, and $D_{aa}^{(0)}$ as given in the Appendix of Ref. [3] but without the renormalization counterterms and using $f_A = 0$. Again, we can write $c_1^{q\bar{q}} = c_{1\,\mu}^{q\bar{q}} + T_1^{q\bar{q}}$ with

$$c_{1\,\mu}^{q\bar{q}} = \ln\left(\frac{\mu_F^2}{s}\right) C_F \left[\ln\left(\frac{tu}{Q_T^4}\right) - \frac{3}{2}\right] + \frac{\beta_0}{4}\ln\left(\frac{\mu_R^2}{s}\right), \qquad (3.18)$$

and $c_2^{q\bar{q}} = c_{2\,\mu}^{q\bar{q}} + T_2^{q\bar{q}}$ with $c_{2\,\mu}^{q\bar{q}} = -2C_F\ln(\mu_F^2/s)$. Finally, another useful notation is $c_1^{q\bar{q}} \equiv c'^{q\bar{q}}_{1\,\mu} + T'^{q\bar{q}}_1$ where $c'^{q\bar{q}}_{1\,\mu}$ is defined as $c_{1\,\mu}^{q\bar{q}}$ with Q_T^2 instead of s in the denominators of the logarithms involving the scales μ_F and μ_R.

The NNLO soft corrections for $q\bar{q} \longrightarrow Wg$ can be written as

$$E_Q \frac{d\hat{\sigma}_{q\bar{q}\to Wg}^{(2)}}{d^3Q} = F_{q\bar{q}\to Wg}^B \frac{\alpha_s^2(\mu_R^2)}{\pi^2}\,\hat{\sigma}'^{(2)}_{q\bar{q}\to Wg} \qquad (3.19)$$

with

$$\begin{aligned}
\hat{\sigma}'^{(2)}_{q\bar{q}\to Wg} =\ & \frac{1}{2}(c_3^{q\bar{q}})^2 \left[\frac{\ln^3(s_2/Q_T^2)}{s_2}\right]_+ + \left[\frac{3}{2}c_3^{q\bar{q}}c_2^{q\bar{q}} - \frac{\beta_0}{4}c_3^{q\bar{q}} + C_A\frac{\beta_0}{8}\right]\left[\frac{\ln^2(s_2/Q_T^2)}{s_2}\right]_+ \\
& + \left\{c_3^{q\bar{q}}c_1^{q\bar{q}} + (c_2^{q\bar{q}})^2 - \zeta_2(c_3^{q\bar{q}})^2 - \frac{\beta_0}{2}T_2^{q\bar{q}} + \frac{\beta_0}{4}c_3^{q\bar{q}}\ln\left(\frac{\mu_R^2}{s}\right) + 2C_F K \right. \\
& \left. + C_A\left[-\frac{K}{2} + \frac{\beta_0}{4}\ln\left(\frac{Q_T^2}{s}\right)\right] - \frac{\beta_0^2}{16}\right\}\left[\frac{\ln(s_2/Q_T^2)}{s_2}\right]_+ \\
& + \left\{c_2^{q\bar{q}}c_1^{q\bar{q}} - \zeta_2 c_2^{q\bar{q}}c_3^{q\bar{q}} + \zeta_3(c_3^{q\bar{q}})^2 - \frac{\beta_0}{2}T_1^{q\bar{q}} + \frac{\beta_0}{4}c_2^{q\bar{q}}\ln\left(\frac{\mu_R^2}{s}\right) + \mathcal{G}_{q\bar{q}}^{(2)} \right. \\
& + C_F\left[\frac{\beta_0}{4}\ln^2\left(\frac{\mu_F^2}{s}\right) - K\ln\left(\frac{\mu_F^2}{s}\right) - K\ln\left(\frac{tu}{Q_T^4}\right)\right] \\
& \left. + C_A\left[\frac{\beta_0}{8}\ln^2\left(\frac{Q_T^2}{s}\right) - \frac{K}{2}\ln\left(\frac{Q_T^2}{s}\right)\right] - \frac{\beta_0^2}{16}\ln\left(\frac{Q_T^2}{s}\right)\right\}\left[\frac{1}{s_2}\right]_+. \qquad (3.20)
\end{aligned}$$

The function $\mathcal{G}_{q\bar{q}}^{(2)}$ denotes again a set of two–loop contributions [9, 10] and is given by

$$\mathcal{G}_{q\bar{q}}^{(2)} = C_F C_A\left(\frac{7}{2}\zeta_3 + \frac{22}{3}\zeta_2 - \frac{299}{27}\right) + n_f C_F\left(-\frac{4}{3}\zeta_2 + \frac{50}{27}\right). \qquad (3.21)$$

Again, we have not included in $\mathcal{G}_{q\bar{q}}^{(2)}$ all two–loop process–dependent contributions.

We also note that we do not calculate the full virtual corrections. The NNLO $\delta(s_2)$ terms that we calculated only include the factorization and renormalization scale dependence and are used in the study of the scale dependence of the NNLO–NNNLL cross section. These terms are:

$$\begin{aligned}
\Bigg\{& \frac{1}{2}(c'^{q\bar{q}}_{1\,\mu})^2 + c'^{q\bar{q}}_{1\,\mu}T'^{q\bar{q}}_1 + \frac{\beta_0}{4}c'^{q\bar{q}}_{1\,\mu}\ln\left(\frac{Q_T^2}{s}\right) + \frac{\beta_0}{4}c_1^{q\bar{q}}\ln\left(\frac{\mu_R^2}{Q_T^2}\right) \\
& - 2C_F^2\zeta_2\ln^2\left(\frac{\mu_F^2}{Q_T^2}\right) + 2C_F\ln\left(\frac{\mu_F^2}{Q_T^2}\right)\left(\zeta_2 T_2^{q\bar{q}} - 2\zeta_2 C_F\ln\left(\frac{Q_T^2}{s}\right) - \zeta_3 c_3^{q\bar{q}}\right) \\
& - \frac{\beta_0^2}{32}\ln^2\left(\frac{\mu_R^2}{Q_T^2}\right) - \frac{\beta_0^2}{16}\ln\left(\frac{\mu_R^2}{Q_T^2}\right)\ln\left(\frac{Q_T^2}{s}\right) + \frac{\beta_1}{16}\ln\left(\frac{\mu_R^2}{Q_T^2}\right) \\
& + \frac{\beta_0}{8}\left[\frac{3}{2}C_F - C_F\ln\left(\frac{tu}{Q_T^4}\right)\right]\left[\ln^2\left(\frac{\mu_F^2}{Q_T^2}\right) + 2\ln\left(\frac{\mu_F^2}{Q_T^2}\right)\ln\left(\frac{Q_T^2}{s}\right)\right] \\
& + C_F\frac{K}{2}\ln\left(\frac{tu}{Q_T^4}\right)\ln\left(\frac{\mu_F^2}{Q_T^2}\right) - 2\gamma'^{(2)}_{q/q}\ln\left(\frac{\mu_F^2}{Q_T^2}\right)\Bigg\}\,\delta(s_2). \qquad (3.22)
\end{aligned}$$

7

4   NUMERICAL RESULTS FOR LARGE-Q_T W PRODUCTION AT THE TEVATRON

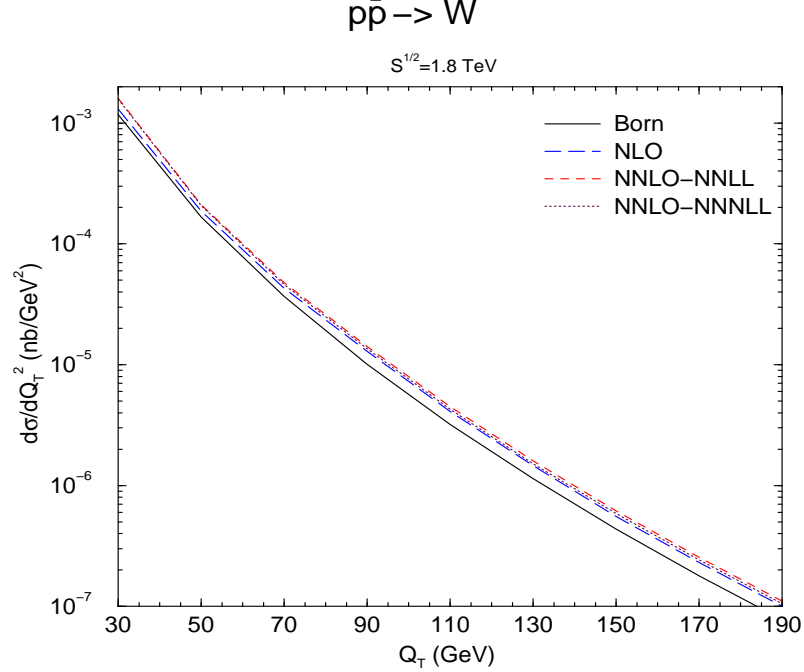

Figure 1: The differential cross section, $d\sigma/dQ_T^2$, for W hadroproduction in $p\bar{p}$ collisions at the Tevatron with $\sqrt{S} = 1.8$ TeV and $\mu_F = \mu_R = Q_T$. Shown are the Born (solid line), NLO (long-dashed line), NNLO–NNLL (short–dashed line), and NNLO–NNNLL (dotted line) results.

We now apply our results to W hadroproduction at large transverse momentum at the Tevatron. Throughout we use the MRST2002 approximate NNLO parton densities [17]. In Fig. 1 we plot the transverse momentum distribution, $d\sigma/dQ_T^2$, for W hadroproduction at Tevatron Run I with $\sqrt{S} = 1.8$ TeV. Here we have set $\mu_F = \mu_R = Q_T$. We plot Born, exact NLO [2, 3], NNLO–NNLL, and NNLO–NNNLL results. We see that the NLO corrections provide a significant enhancement of the Born cross section. The NNLO–NNLL corrections provide a further modest enhancement of the Q_T distribution. If we increase the accuracy by including the NNNLL contributions, which are negative, then we find that the NNLO–NNNLL cross section lies between the NLO and NNLO–NNLL results. Similar results are shown for W hadroproduction at Tevatron Run II with $\sqrt{S} = 1.96$ TeV in Fig. 2.

Since it is hard to distinguish between the various curves in figures 1 and 2, we provide two more figures, Fig. 3 and Fig. 4, for Run I and II respectively, which emphasize the very high–Q_T region where the soft–gluon approximation holds best.

In Fig. 5 we plot the K–factors, i.e. the ratios of cross sections at various orders and accuracies to the Born cross section, all with $\mu_F = \mu_R = Q_T$, in the high–Q_T region of W production at Tevatron Run I. Shown are the K–factors for exact NLO/Born (long–dashed line), NLO–NLL/Born (dash–dotted line), NNLO–NNLL/Born (short–dashed line), and approximate NNLO–NNNLL/Born (dotted line) results. We also show the ratio of the exact NLO to the NLO–NLL cross section. It is clear from this line being very close to 1 that the NLO–NLL result is a very good approximation to the full NLO result, i.e. the soft–gluon corrections overwhelmingly dominate the NLO cross section. The difference between
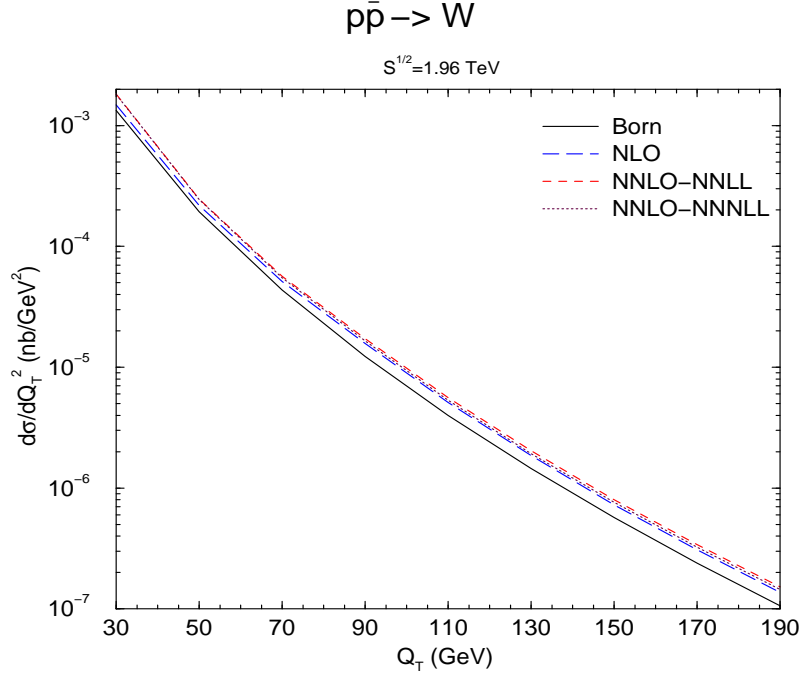
Figure 2: The differential cross section, $d\sigma/dQ_T^2$, for W hadroproduction in $p\bar{p}$ collisions at the Tevatron Run II with $\sqrt{S} = 1.96$ TeV and $\mu_F = \mu_R = Q_T$. Shown are the Born (solid line), exact NLO (long–dashed line), NNLO–NNLL (short–dashed line), and NNLO–NNNLL (dotted line) results.

NLO and NLO–NLL is only 2% for $Q_T > 90$ GeV and less than 10% for lower Q_T down to 30 GeV. The fact that the soft–gluon corrections dominate the NLO cross section is a major justification for studying the NNLO soft gluon corrections to this process. We can also see that the various K–factors shown in Fig. 5 are moderate, and nearly constant over the Q_T range shown even though the distributions themselves span two orders of magnitude in this range. The NLO corrections are nearly 30% over the Born, with the NNLO corrections giving an additional increase, so that the NNLO–NNLL/Born K–factor is around 1.4 and the NNLO–NNNLL/Born K–factor is around 1.35. We note that the K–factors for Run II are very similar.

In Fig. 6 we plot the scale dependence of the differential cross section for W production at Tevatron Run I for $Q_T = 80$ GeV. We define $\mu \equiv \mu_F = \mu_R$ and plot the differential cross section versus μ/Q_T over two orders of magnitude: $0.1 < \mu/Q_T < 10$. We note the good stabilization of the cross section when the NLO corrections are included, and the further improvement when the NNLO–NNNLL corrections (which include all the soft and virtual NNLO scale terms) are added. The NNLO–NNNLL result approaches the scale independence expected of a truly physical cross section.

In Fig. 7 we plot the differential cross section $d\sigma/dQ_T^2$ at high Q_T with $\sqrt{S} = 1.8$ TeV for two values of scale, $Q_T/2$ and $2Q_T$, often used to display the uncertainty due to scale variation. We note that while the variation of the Born cross section is significant, the variation at NLO is much smaller, and at NNLO–NNNLL it is very small. In fact the two NNLO–NNNLL curves lie on top of the $\mu = Q_T/2$ Born curve, and so does the NLO $\mu = Q_T/2$ curve. These results are consistent with Fig. 6. In Fig. 8 we show analogous results for Run II.
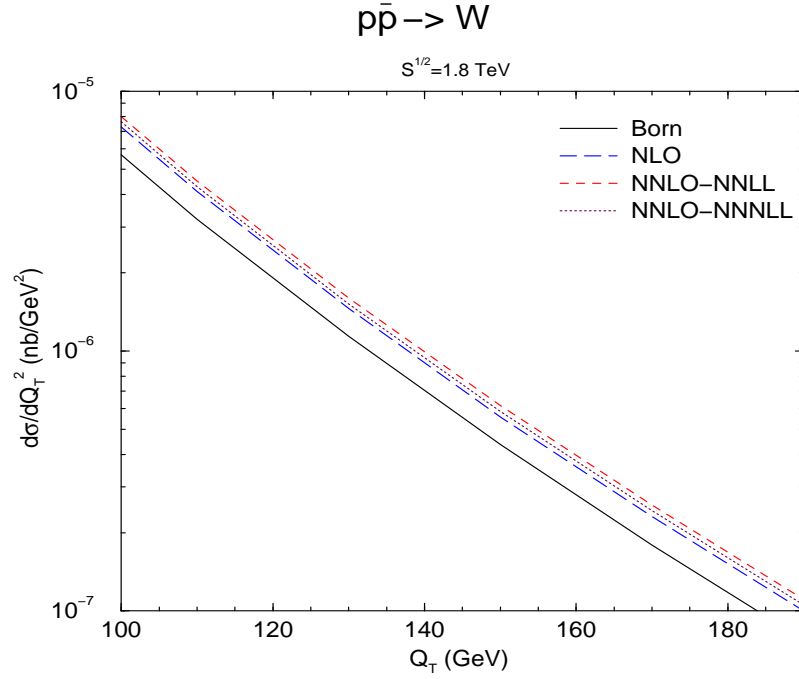
Figure 3: The differential cross section, $d\sigma/dQ_T^2$, of Fig. 1 at high Q_T. The labels are the same as in Fig. 1.

5   CONCLUSION

The NNLO soft–gluon corrections for W hadroproduction at large transverse momentum in $p\bar{p}$ collisions have been presented, in particular for the case of the Tevatron Run I and II. It has been shown that the NLO soft–gluon corrections fully dominate the NLO differential cross section at large transverse momentum, and that the NNLO soft–gluon corrections provide modest enhancements while further decreasing the factorization and renormalization scale dependence of the transverse momentum distributions as expected in any consistent perturbative expansion.

References

[1] Ellis,R.K.;Veseli,S. Phys. Rev. 1999, D60, 011501.

[2] Arnold,P.B.;Reno,M.H. Nucl. Phys. 1989, B319, 37; (E) 1990, B330, 284.

[3] Gonsalves,R.J.;Pawlowski,J.;Wai,C.-F. Phys. Rev. 1989, D40, 2245; Phys. Lett. 1990, B252, 663.

[4] Kidonakis,N.;Sterman,G. Phys. Lett. 1996, B387, 867; Nucl. Phys. 1997, B505, 321.

[5] Kidonakis,N.;Oderda,G.;Sterman,G. Nucl. Phys. 1998, B525, 299; 1998, B531, 365.

[6] Laenen,E; Oderda,G.; Sterman,G. Phys. Lett. 1998, B438, 173.

[7] Kidonakis,N. Int. J. Mod. Phys. 2000, A15, 1245; Mod. Phys. Lett. 2004, A19, 405.

[8] Kidonakis,N.;Del Duca,V. Phys. Lett. 2000, B480, 87; Kidonakis,N. in *Proceedings of the EPS-HEP99 Conference*, p. 392, hep-ph/9910240.
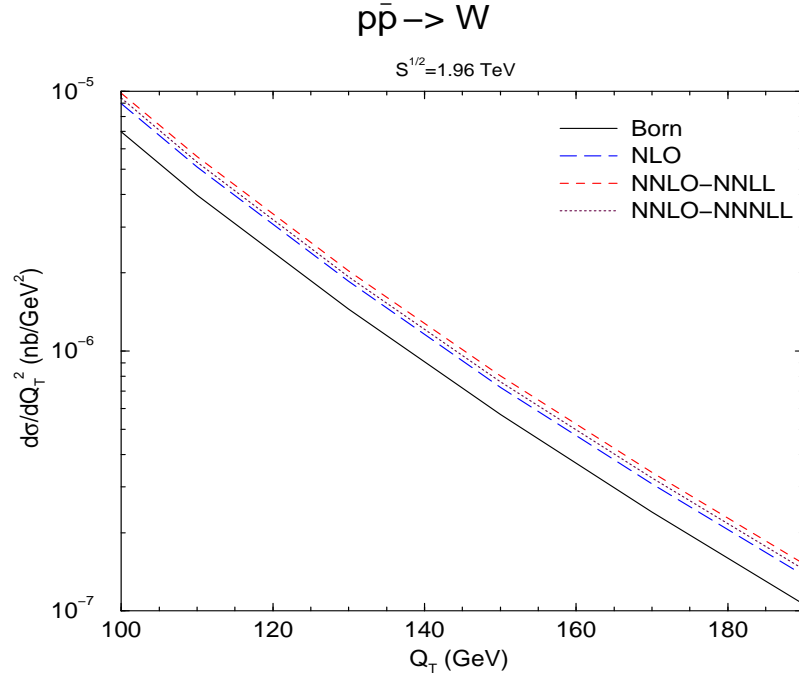
Figure 4: The differential cross section, $d\sigma/dQ_T^2$, of Fig. 2 at high Q_T. The labels are the same as in Fig. 2.

[9] Kidonakis,N. Int. J. Mod. Phys. 2004, A19, 1793; in *DIS03*, hep-ph/0306125, hep-ph/0307207.

[10] Kidonakis,N.;Sabio Vera,A. JHEP 2004, 0402, 027; in *DIS04*, hep-ph/0405013; in *DPF2004*, hep-ph/0409206.

[11] Kidonakis,N.;Owens,J.F. Phys. Rev. 2000, D61, 094004; Int. J. Mod. Phys. 2004, A19, 149; Kidonakis,N. Nucl. Phys. (Proc. Suppl.) 1999, B79, 410.

[12] Kodaira,J.;Trentadue,L. Phys. Lett. 1982, 112B, 66.

[13] Gonzalez-Arroyo,A.;Lopez,C.;Yndurain,F.J. Nucl. Phys. 1979, B153, 161.

[14] Curci,G.;Furmanski,W.;Petronzio,R. Nucl. Phys. 1980, B175, 27; Furmanski,W.;Petronzio,R. Phys. Lett. 1980, 97B, 437.

[15] Kidonakis,N. hep-ph/0208056; in *DIS03*, hep-ph/0307145.

[16] Kidonakis,N. Phys. Rev. 2001, D64, 014009; Kidonakis,N.;Vogt,R. Phys. Rev. 2003, D68, 114014; Eur. Phys. J. 2004, C33, s466.

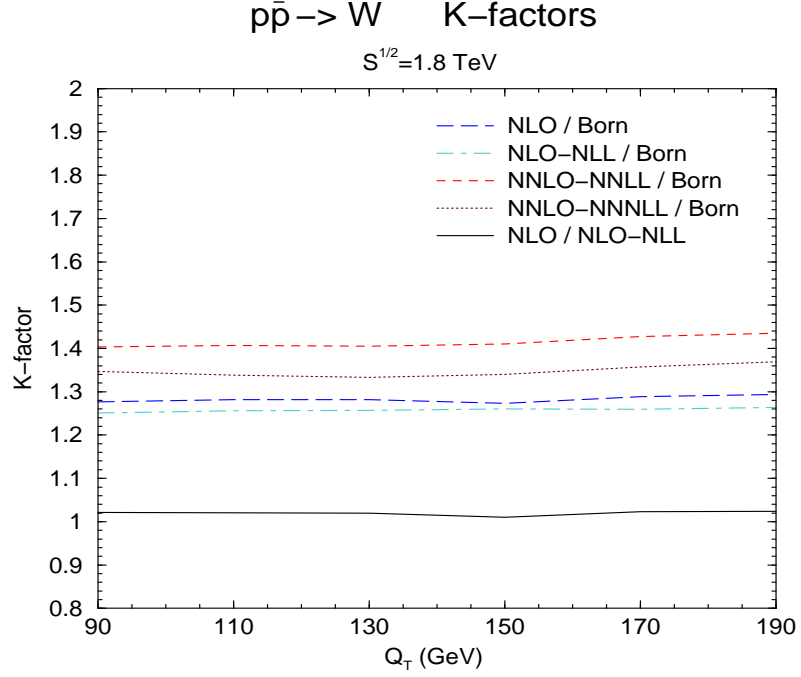[17] Martin,A.D.;Roberts,R.G.;Stirling,W.J.;Thorne,R.S. Eur. Phys. J. 2003, C28, 455.

Figure 5: The K–factors for the differential cross section, $d\sigma/dQ_T^2$, for W hadroproduction in $p\bar{p}$ collisions at the Tevatron with $\sqrt{S} = 1.8$ TeV and $\mu_F = \mu_R = Q_T$.
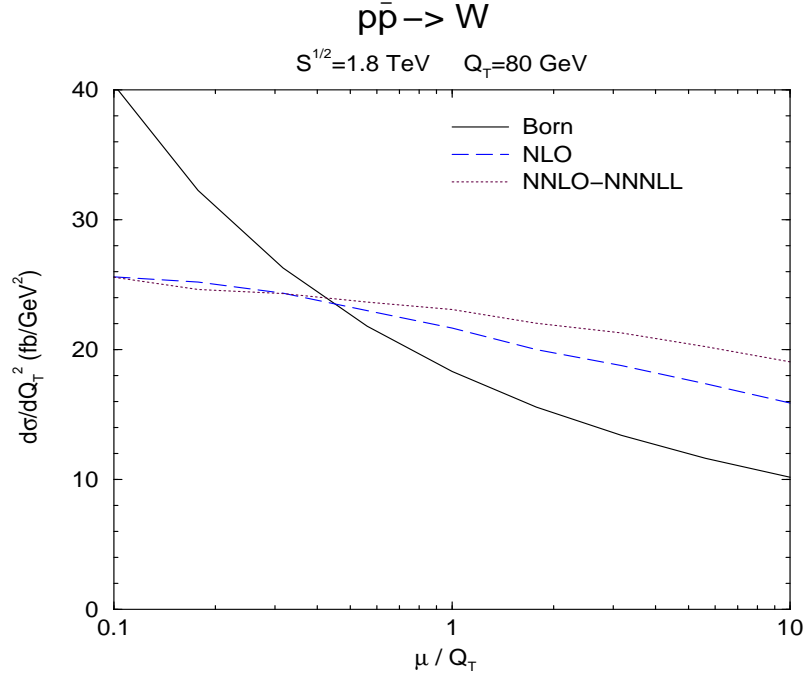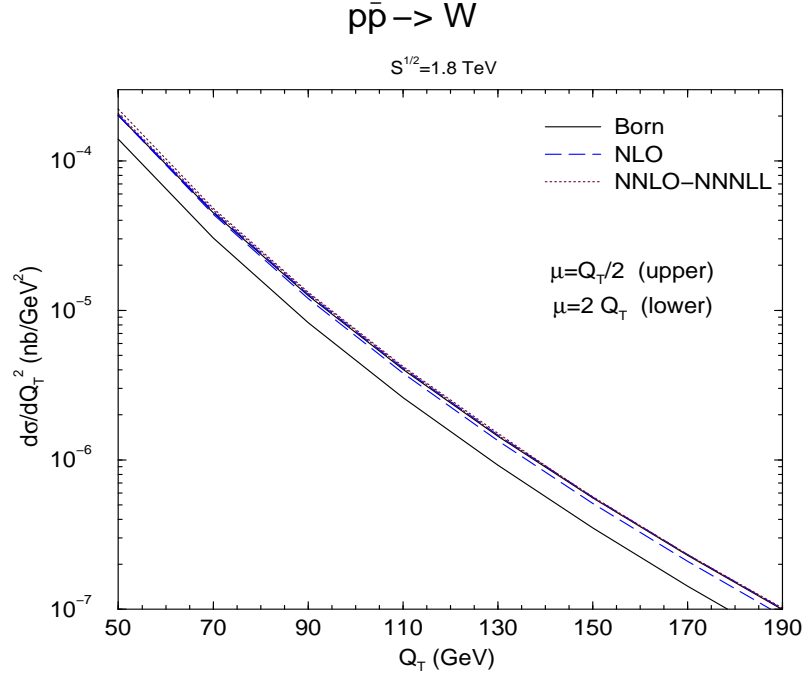

Figure 6: The differential cross section, $d\sigma/dQ_T^2$, for W hadroproduction in $p\bar{p}$ collisions at the Tevatron with $\sqrt{S} = 1.8$ TeV, $Q_T = 80$ GeV, and $\mu \equiv \mu_F = \mu_R$. Shown are the Born (solid line), exact NLO (long–dashed line), and NNLO–NNNLL (dotted line) results.

12

pp̄ –> W

S^(1/2)=1.8 TeV

Figure 7: The differential cross section, $d\sigma/dQ_T^2$, for W hadroproduction in $p\bar{p}$ collisions at the Tevatron with $\sqrt{S} = 1.8$ TeV and $\mu \equiv \mu_F = \mu_R = Q_T/2$ or $2Q_T$. Shown are the Born (solid lines), NLO (long–dashed lines), and NNLO–NNNLL (dotted lines) results. The upper lines are with $\mu = Q_T/2$, the lower lines with $\mu = 2Q_T$.
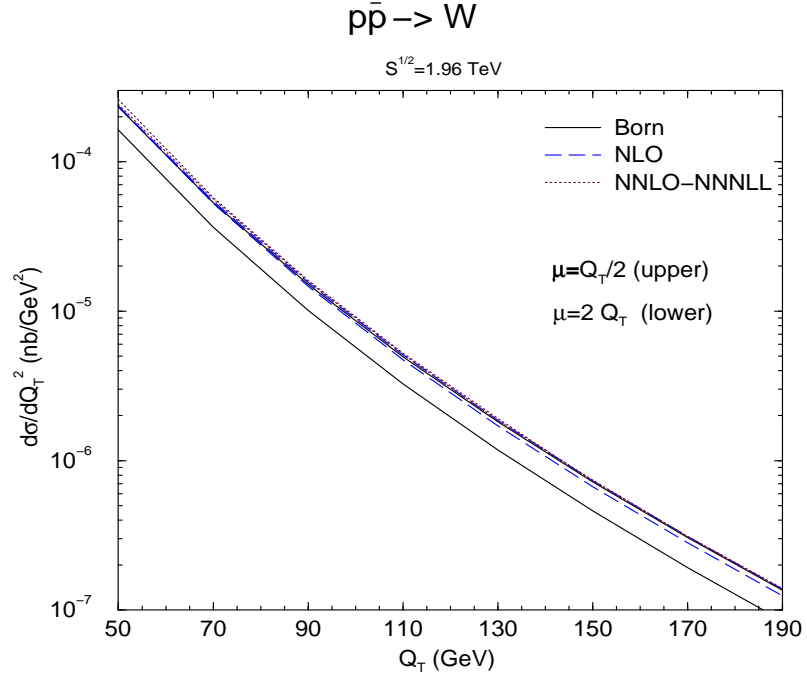
pp̄ –> W

S^(1/2)=1.96 TeV

Figure 8: The differential cross section, $d\sigma/dQ_T^2$, for W hadroproduction in $p\bar{p}$ collisions at the Tevatron with $\sqrt{S} = 1.96$ TeV and $\mu \equiv \mu_F = \mu_R = Q_T/2$ or $2Q_T$. The labels are as in Fig. 7.